ELSEVIER

Thermochimica Acta 383 (2002) 79–85

thermochimica acta

www.elsevier.com/locate/tca

Thermogravimetric estimation of adsorption properties of europium-incorporated MCM-41 materials

Lucildes P. Mercuri[a,b], Jivaldo R. Matos[a,b], Mietek Jaroniec[a,*]

[a]*Department of Chemistry, Kent State University, Kent, OH 44242, USA*
[b]*Instituto de Química da Universidade de São Paulo, C.P. 26.077, 05599-970, São Paulo, SP, Brazil*

Received 31 January 2001; received in revised form 25 June 2001; accepted 25 June 2001

Abstract

This work reports the study of *n*-butanol thermodesorption from Eu(1, 3 and 5%)-incorporated MCM-41 samples, which was done to verify the thermogravimetric (TG) method for estimation of adsorption properties such as the specific surface area and the volume of primary mesopores for nanoporous materials. The materials studied were synthesized under hydrothermal conditions using a surfactant templating route. The high-resolution TG/1st DTG/2nd DTG curves were obtained in the range from room temperature to 300 °C with heating rate of 5 °C/min in flowing nitrogen. The values of the mesopore volume and specific surface area obtained from the TG data are in good agreement with those evaluated from low-temperature nitrogen adsorption isotherms. In addition, this study shows the importance of the 1st DTG and 2nd DTG curves in the evaluation of the mesopore volume and specific surface area for ordered mesoporous materials. © 2002 Elsevier Science B.V. All rights reserved.

Keywords: High-resolution thermogravimetry; Europium-incorporated MCM-41; *n*-Butanol thermodesorption; Mesopore volume; Specific surface area

1. Introduction

The discovery of ordered mesoporous materials (OMMs) [1], such as MCM-41, opened new perspectives and created new challenges in the field of characterization of adsorbents and catalysts using gas adsorption. These well-defined structures can be considered as model solids [2–8] to verify both new and previously developed characterization methods and to either validate them for general or specific application [7,8].

OMMs have been synthesized under hydrothermal conditions with a liquid crystal templating mechanism [1,9,10]. Their pore sizes may be adjusted from 2 to 10 nm by using a proper surfactant [1,9], addition of expander molecules during synthesis [1,11] and/or specific post-synthesis treatment [12–14]. Structural and surface properties of OMMs can be evaluated by several methods including adsorption, which plays an important role in their characterization [8,15]. For instance, adsorption–desorption isotherms are commonly used to determine the BET specific surface area, external surface area, and volumes of primary and secondary mesopores as well as their sizes and distributions [8,15].

The incorporation of heteroatoms into the MCM-41 framework has been used to alter both the structural

---

[*] Corresponding author. Tel.: +1-330-672-3790;
fax: +1-330-672-3816.
E-mail address: jaroniec@columbo.kent.edu (M. Jaroniec).

PII: S0040-6031(01)00677-3

ordering and hydrothermal stability of the resulting materials [16]. Currently there is considerable interest in the synthesis and hydrothermal stability of heteroatom-containing mesoporous silicas [17]. Although some analytical methods such as powder X-ray diffraction (XRD) and transmission electron microscopy have been used to identify the type of structural ordering in these materials, each of them has its limitations and provides information only about local scale of the structure ordering in OMMs [15].

Gas adsorption is an excellent technique for characterization of the global structural and surface properties of OMMs. Accurate adsorption measurements often require special analysis conditions and are time-consuming [15,18]. Because of this, there is a great interest in the development of new methods to characterize the structural and surface properties of nanoporous solids [19].

Among several thermal analysis techniques, thermogravimetry is one of the most promising methods to investigate the surface and sorption properties of solid materials. The principle of thermogravimetry is to record the change in the sample weight (loss or gain) as a function of temperature and/or time [20]. The resulting weight-change curve (TG curve) versus temperature or time provides information about the thermal stability and composition of the initial sample as well as the thermal stability and composition of any intermediate compounds that may be formed. In addition, the DTG curve, i.e. the derivative of the weight-change of the sample with respect to time, d*m*/d*t*, is obtained as a function of time (*t*) or temperature (*T*). The DTG curve does not provide more information than the TG curve; it simply provides another way for displaying data and facilitates their qualitative and quantitative interpretation [20,21]. It is advantageous to present the DTG curve in conjunction with the TG curve. Such presentation of TG data facilitates the determination of the "characteristic" temperatures at the beginning, maximum and end of a given weight change as well as the detection of the TG events.

The introduction of high-resolution thermogravimetric analyzers (HR TG) increased the interest in characterization of the surface properties of new materials because of their capability to monitor the stepwise thermodesorption of adsorbed molecules from porous solids [22]. In this mode the heating rate is automatically adjusted in response to the weight change of the sample in order to maximize the resolution. Previous studies [23–27] showed a great utility of HR TG for characterization of porous materials including active carbons and silica gels.

The objective of this work was to study the thermodesorption of *n*-butanol from Eu(1, 3 and 5%)-incorporated MCM-41 to verify the TG method for evaluation of the specific surface area and the volume of primary mesopores. This method can be used for a quick characterization of ordered mesoporous solids. Also, it is shown that the 1st DTG and 2nd DTG curves are very useful for quantitative interpretation of the TG thermodesorption data, and consequently for evaluation of the mesopore volume and specific surface area of OMMs.

2. Experimental

2.1. Materials synthesis

The samples denoted as Eu*X*-MCM-41 (where *X* refers to percentage of Eu^{3+} used in the MCM-41 synthesis) materials were synthesized via a hydrothermal method similar to that reported in [28]. Cab-O-Sil M-5 silica (Cabot Co.), Eu_2O_3 (Sigma), chloric acid (Fisher Scientific), cetyltrimethylammonium bromide (CTMABr) as the template (Aldrich) and 97% tetramethylammonium hydroxide pentahydrate ($TMAOH{\cdot}5H_2O$) as a mineralizer (Fisher Scientific) were used to synthesize the Eu-incorporated MCM-41 samples. The synthesis procedure reported in [28] was slightly modified in the current work. All reactants were used as received and mixed according with the following molar composition: $1.0SiO_2{:}0.317TMAOH{:}0.45CTMABr{:}xEu_2O_3{:}67H_2O$ ($x = 0.005$, 0.015 and 0.025). In a typical synthesis of Eu(3%)-incorporated MCM-41, $TMAOH{\cdot}5H_2O$ (1.48 g) was dissolved in 20.0 g of water and 4.09 g of CTMABr was added into TMAOH solution under vigorous mechanical stirring (pH = 13.5). Then, 0.132 g of Eu_2O_3 was dissolved in 3.5 g of 2 M HCl solution and added into the TMAOH–CTMABr mixture. The remaining amount of water was added to the synthesis mixture to achieve the mass of 30.1 g (pH = 12.8). After 15 min of stirring, 1.5 g of the Cab-O-Sil silica was added and the stirring was continued for next 30 min (pH = 12.5). The resulting gel was transferred into a Teflon-lined autoclave, and heated statically under autogenous pressure for 40 h at 100 °C. After cooling to room temperature, the resulting solid product (pH $= 12.2$) was filtered and washed extensively with deionized water and dried at room temperature. The samples were calcined in flowing nitrogen (100 ml min^{-1}) from room temperature to 540 °C using a heating rate of 1 °C min^{-1}. After heating for 5 h at 540 °C, the flowing gas was switched from nitrogen to air and the heating was kept isothermal for an additional 2 h.

2.2. Nitrogen adsorption measurements

Prior to adsorption measurements each sample was degassed at 200°C for at least 2 h until a pressure of 10^{-4} Pa was attained. Adsorption–desorption isotherms of nitrogen were measured on an ASAP-2010 model volumetric adsorption analyzer (Micromeritcs, Norcross, GA) at −196°C over a relative pressure range ca. 10^{-6} to 0.995. The specific surface area was determined according to the standard Brunauer–Emmett–Teller (BET) method [29], and the total pore volume was obtained according to the single point method [30]. The α_s-plot method [31] was employed to assess the porosity of the samples and estimate the volume and surface area of mesopores. The pore size distribution was obtained by the Barrett–Joyner–Halenda (BJH) method [32] recently modified by Kruk et al. [8].

2.3. Thermogravimetric measurements

TG/1st DTG/2nd DTG curves for the systems studied were obtained on a Model TG 2950 high-resolution thermogravimetric analyzer from TA Instruments (New Castle, DE) equipped with a platinum crucible and an automatically programmed temperature controller. All measurements were carried out under nitrogen atmosphere (60 ml min^{-1}) using the sample mass between 6 and 8 mg from room temperature to 300 °C with maximum heating rate of 5 °C min^{-1} to remove the physically adsorbed species. After each TG run of the blank samples, the furnace was slowly cooled to 34 °C and after opening, the sample was unloaded to add two drops of *n*-butanol, and quickly loaded into the HR TG instrument. After closing the furnace the sample was allowed to equilibrate for 10 min. Next, the furnace was opened to check the sample, and if it seemed to be dry one drop of *n*-butanol was added. Subsequently, the *n*-butanol thermodesorption was measured up to 300 °C with maximum heating rate of 5 °C min^{-1}. This experimental procedure is analogous to that reported previously [33].

3. Results and discussion

3.1. Nitrogen adsorption studies

Nitrogen adsorption–desorption isotherms at −196 °C for pure MCM-41 and Eu(1, 3 and 5%)-incorporated MCM-41 samples are shown in Fig. 1. All samples exhibit similar isotherms with a distinct step in the relative pressure (p/p_0) range from 0.2 to 0.4, which reflects the capillary condensation (filling) of nitrogen in cylindrical mesopores. A significant increase in the amount of adsorbed nitrogen is

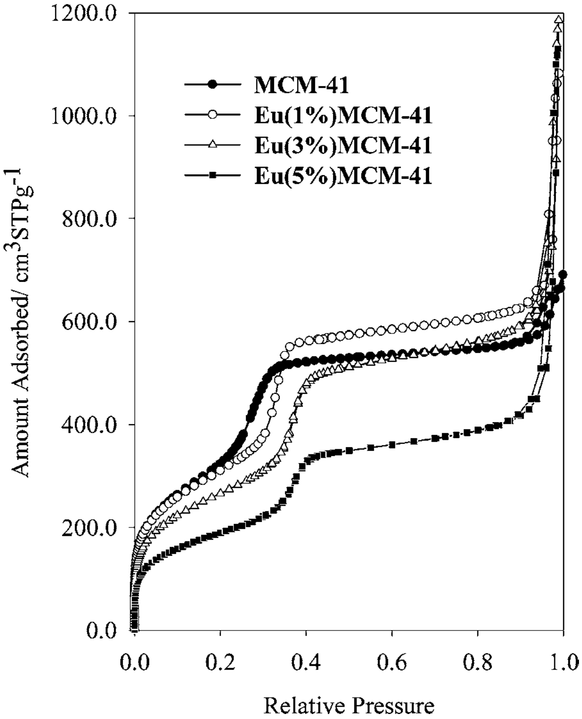

Fig. 1. Nitrogen adsorption isotherms for pure MCM-41 and Eu(1, 3 and 5%)-incorporated MCM-41 materials at −196 °C.

Table 1
Comparison of the volumes of primary mesopores and the specific surface areas obtained from the *n*-butanol thermodesorption TG data and nitrogen adsorption for the pure MCM-41 and Eu(1, 3 and 5%)-incorporated MCM-41 samples[a]

Sample	Method			
	N_2 adsorption data		*n*-Butanol HR TG data	
	S_{BET} (m^2/g)	V_P (cm^3/g)	$S_{butanol}$ (m^2/g)	V_P (cm^3/g)
MCM-41	1120	0.77	986	0.72
Eu(1%)-incorporated MCM-41	1094	0.80	1141	0.83
Eu(3%)-incorporated MCM-41	944	0.65	940	0.68
Eu(5%)-incorporated MCM-41	671	0.42	703	0.52

[a] S_{BET}: BET specific surface area from nitrogen adsorption; $S_{butanol}$: specific surface area from the TG data; V_P: the volume of primary mesopores.

observed for relative pressures greater than 0.8 indicating the presence of secondary mesopores in the porous structure of the resulting MCM-41 materials. The contribution of the secondary mesoporosity seems to increase with increasing percentage of Eu. The volumes of primary mesopores and specific surface areas evaluated from nitrogen adsorption isotherms for all samples studied are summarized in Table 1. The specific surface areas of the Eu(1, 3 and 5%)-incorporated MCM-41 samples are smaller in comparison to that for pure MCM-41 material. It seems that the introduction of Eu into the MCM-41 structure decreases its specific surface area (see Table 1) and increases the size of primary mesopores because the condensation step shifts in the direction of higher relative pressures [8,15].

3.2. Thermogravimetric studies

The high-resolution TG/1st DTG/2nd DTG curves obtained for *n*-butanol thermodesorption were recorded to evaluate the volume of primary mesopores and the specific surface area of the samples studied. The TG/1st DTG/2nd DTG curves plotted as a function of temperature are shown in Fig. 2. All the samples show similar TG profiles. As in [33] the identification of the TG events related to thermodesorption of *n*-butanol from the samples was done by using TG/1st DTG/2nd DTG curves plotted as a function of time because in HR TG temperature is not a linear function of time due to the variable-heating rate. Fig. 3 shows the TG/1st DTG/2nd DTG curves plotted as a function of time of all the samples studied. All 1st DTG and 2nd DTG curves

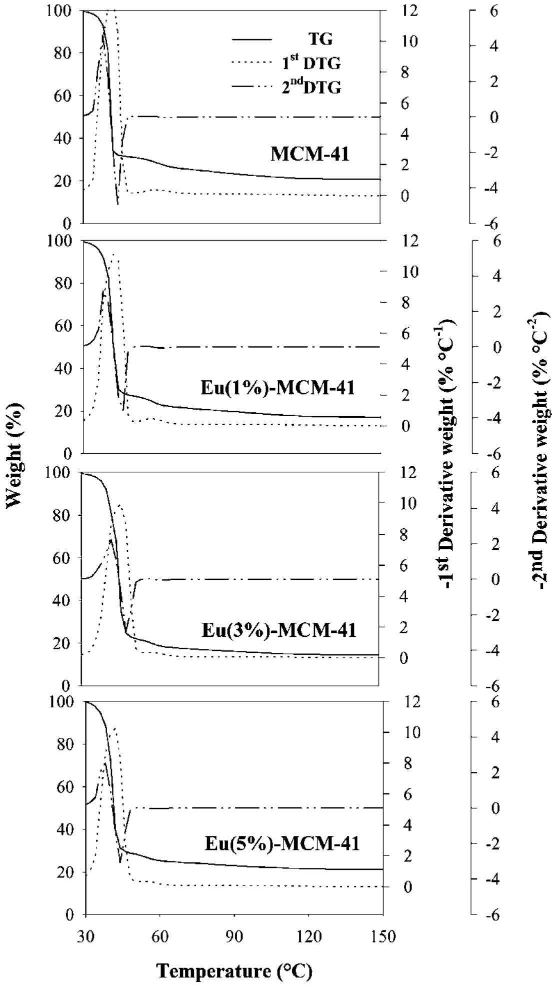

Fig. 2. The TG/1st DTG/2nd DTG curves as a function of temperature for pure MCM-41 and Eu(1, 3 and 5%)-incorporated MCM-41 samples immersed with *n*-butanol.

exhibit four TG events, the last three of which are well defined. The first event occurs around 40 °C and reflects the evaporation of the excess *n*-butanol. The second event occurs between 40 and 60 °C and corresponds to the amount of thermodesorbed *n*-butanol from the interior of mesopores, which after conversion gives the volume of primary mesopores. The third and fourth events occur consecutively between ca. 60 and 170 °C and correspond to the monolayer capacity of the sample (gradual thermodesorption of probe molecules from the mesopore walls), which after conversion gives the specific surface area. It should be noted here the importance of the 1st DTG and 2nd DTG curves in the determination of the volume of primary mesopores

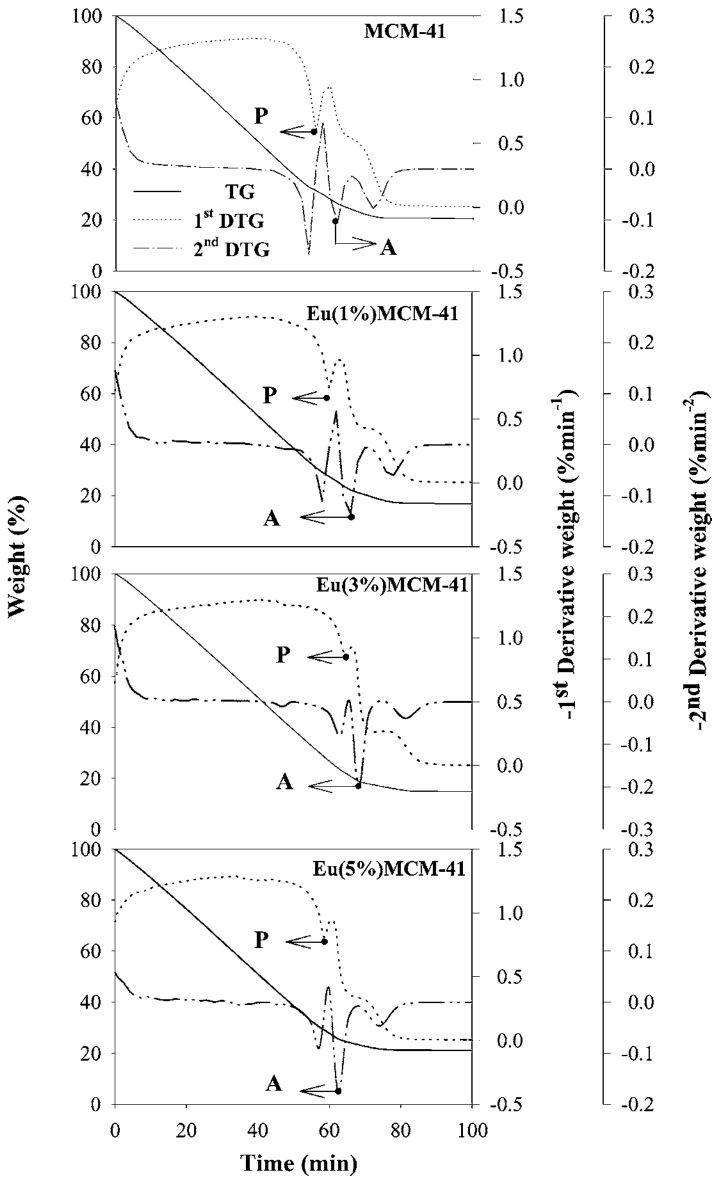

Fig. 3. The TG/1st DTG/2nd DTG curves as a function of time for pure MCM-41 and Eu(1, 3 and 5%)-incorporated MCM-41 samples immersed with *n*-butanol.

and specific surface area. As can be seen in Fig. 3, the 1st DTG curve shows the point 'P' that corresponds to the mass, which after the residue subtraction is equal to the adsorption capacity of mesopores. The following equation was used to convert this capacity into the volume of primary mesopores, V_P:

$$V_P = \left(\frac{V}{M}\right)\left(\frac{m_P}{m_R}\right) \quad (1)$$

where V is the molar volume of liquid *n*-butanol, M the molar mass of the adsorbate, m_P the weight loss and m_R is the residue mass. On the other hand, the 2nd DTG curve shows the point A, which indicates the weight loss m_A that can be converted the specific surface area (S) of the sample. The following expression was used to calculate the specific surface area:

$$S = \frac{m_A N_A \omega}{M m_R} \quad (2)$$

where N_A is the Avogadro number and ω is the cross-sectional area of adsorbate molecule. The *n*-butanol molar volume of 98.7 cm^3/mol and cross-sectional area of 40×10^{-20} m^2 per molecule were used in calculations [27,33]. The values of V_P and S calculated on the basis of the TG measurements are listed in Table 1 and compared with those obtained from nitrogen adsorption.

4. Conclusions

The first and second derivatives of the time-dependent weight-change of the pure MCM-41 and Eu(1, 3 and 5%)-incorporated MCM-41 samples saturated with *n*-butanol facilitated the TG data analysis, which allows for determination of the volume of primary mesopores and specific surface area of the OMMs studied. These values are in good agreement with the corresponding values obtained by nitrogen adsorption. The current work demonstrates the great importance of HR TG for characterization of ordered mesoporous materials.

Acknowledgements

L.P.M. and J.R.M. are grateful to the Fundação de Amparo à Pesquisa do Estado de São Paulo (FAPESP) for the fellowships under Grants 99/11170-5 and 99/11171-1. M.J. gratefully acknowledges the donors of Petroleum Research Fund administered by the American Chemical Society for support of this research.

References

[1] J.S. Beck, J.C. Vartuli, W.J. Roth, M.E. Leonowicz, C.T. Kresge, K.D. Schmitt, C.T.W. Chu, D.H. Olson, E.W. Sheppard, S.B. McCullen, J.B. Higgins, J.L. Schlenker, J. Am. Chem. Soc. 114 (1992) 10834.

[2] O. Franke, G. Schulz-Ekloff, J. Rathousky, J. Starek, A. Zukal, J. Chem. Soc., Chem. Commun. (1993) 724.

[3] P.J. Branton, P.G. Hall, K.S.W. Sing, H. Reichert, F. Schuth, K.K. Unger, J. Chem. Soc., Faraday Trans. 90 (1994) 2965.

[4] P.L. Llewellyn, Y. Grillet, F. Schuth, H. Reichter, K.K. Unger, Micropor. Mater. 3 (1994) 345.

[5] P.I. Ravikovitch, S.C. O'Domhnaill, A.V. Neimark, F. Schuth, K.K. Unger, Langmuir 11 (1995) 4765.

[6] H. Naono, M. Hakuman, T. Shiono, J. Colloid Interface Sci. 186 (1997) 360.

[7] M. Kruk, M. Jaroniec, A. Sayari, J. Phys. Chem. B 101 (1997) 583.

[8] M. Kruk, M. Jaroniec, A. Sayari, Langmuir 13 (1997) 6267.

[9] C.T. Kresge, M.E. Leonowicz, W.J. Roth, J.C. Vartuli, J.S. Beck, Nature 359 (1992) 710.

[10] J.Y. Ying, C.P. Mehnert, M.S. Wong, Angew. Chem. 38 (1999) 56.

[11] Q. Huo, D.I. Margolese, G.D. Stucky, Chem. Mater. 8 (1996) 1147.

[12] D. Klushalani, A. Kuperman, G.A. Ozin, K. Tanak, J. Garces, M. Olken, N. Coombs, Adv. Mater. 7 (1995) 842.

[13] A. Sayari, M. Kruk, M. Jaroniec, Chem. Mater. 9 (1997) 2499.

[14] A. Sayari, M. Kruk, M. Jaroniec, I. Moudrakovski, Adv. Mater. 10 (1998) 1376.

[15] M. Jaroniec, M. Kruk, A. Sayari, Stud. Surf. Sci. Catal. 117 (1998) 325.

[16] K. Moller, T. Bein, Chem. Mater. 10 (1998) 2950.

[17] R. Mokaya, J. Phys. Chem. B 104 (2000) 8279.

[18] S.J. Gregg, K.S.W. Sing, Adsorption, Surface Area and Porosity, Academic Press, London, 1982.

[19] J. Choma, M. Jaroniec, Chem. Anal. (Warsaw) 40 (1995) 175.

[20] W.W. Wendlandt, Thermal Analysis, 3rd Edition, Wiley, New York, 1986.

[21] C.J. Keattch, D. Dollimore, An Introduction to Thermogravimetry, 2nd Edition, Heyden, New York, 1975.

[22] P. Staszczuk, R. Dobrowolski, M. Jaroniec, Langmuir 8 (1992) 229.

[23] M. Jaroniec, R.K. Gilpin, P. Staszczuk, J. Choma, Stud. Surf. Sci. Catal. 87 (1994) 613.

[24] M. Jaroniec, R.K. Gilpin, J. Ramler, J. Choma, Thermochim. Acta 272 (1996) 65.

[25] D. Pan, M. Jaroniec, J. Klinik, Carbon 34 (1996) 1109.

[26] Z. Li, M. Jaroniec, J. Colloid Interface Sci. 210 (1999) 200.

[27] A.S. Araujo, M. Jaroniec, Thermochim. Acta 345 (2000) 173.

[28] A. Sayari, Y. Yang, J. Phys. Chem. B 104 (2000) 4835.

[29] S. Brunauer, P.H. Emmett, E. Teller, J. Am. Chem. Soc. 60 (1938) 309.

[30] M. Jaroniec, in: T.J. Pinnavaia, M.F. Thorpe (Eds.), Access to Nanoporous Materials, Plenum Press, New York, 1996, p. 255.

[31] M. Jaroniec, K. Kaneko, Langmuir 13 (1997) 6589.

[32] E.P. Barrett, L.J. Joyner, P.P. Halenda, J. Am. Chem. Soc. 73 (1951) 373.

[33] D. Pan, M. Jaroniec, Langmuir 12 (1996) 3665.